Journal of Cellular Biochemistry 59:498–513 (1995)

Nuclear Domain 10 (ND10) Associated Proteins Are Also Present in Nuclear Bodies and Redistribute to Hundreds of Nuclear Sites After Stress

Gerd G. Maul, Eunsil Yu, Alexander M. Ishov, and Alan L. Epstein

The Wistar Institute, Philadelphia, Pennsylvania 19104 (G.G.M., E.Y., A.M.I.);
University of Southern California, Los Angeles, California 90033 (A.L.E.)

Abstract The promyelocytic leukemia protein fused to the retinoic acid receptor α in t(15;17) acute promyelocytic leukemia, the primary biliary cirrhosis autoantigen, Sp100, as well as the incompletely characterized protein NDP55, are co-localized in specific immunohistochemically defined nuclear domains (ND10), which are potential equivalents of ultrastructurally defined nuclear bodies. We investigated whether the distribution of these proteins depends on environmental conditions and whether ND10 correlate with nuclear bodies. Certain nuclear bodies and ND10 react in a similar way and share antigens. Interferon exposure doubled the number of ND10 and increased the frequency of nuclear bodies, whereas herpes simplex virus infection or heat shock modify both. Redistribution of ND10-associated proteins to hundreds of small sites throughout the chromatin was inducible by stress in the form of heat shock and exposure to Cd^{++} ions. The change of distribution was rapid and independent of protein synthesis, and thus not part of the classical heat shock response. The very rapid redistribution of these proteins after heat shock, together with the development of ND10 upon interferon activation, raises the possibility that ND10 represent storage sites of certain matrix proteins readily accessible throughout the chromatin in response to stress or other effectors that induce global nuclear changes.

Key words: nuclear bodies, promyelocytic leukemia protein, herpes simplex virus

The cell nucleus at the ultrastructural level seems only crudely compartmentalized into nucleolus, hetero-, and euchromatin. However, the use of probes that localize proteins or RNA species has revealed functional domains in the nucleus, such as areas of concentrated splicing components, that are not observed by electron microscopy (EM) [Carmo-Fonseca et al., 1992; Carter et al., 1991; Fakan et al., 1984; Fu and Maniatis, 1990; Lerner et al., 1981; Spector, 1990]. We have recently characterized nuclear domains that are precisely circumscribed, and because of their frequency designated them as ND10 [Ascoli and Maul, 1991]. ND10 are approximately 0.5 μm in size, corresponding to the size of structures named nuclear bodies by Weber and Frommes [1963] and defined by early electron microscopists as "dense granular bodies and pale round structures, at times showing a complex lamellar pattern" [deThé et al., 1960; Hinglais-Guillaud et al., 1961]. Increased frequency in response to estrogen [Brasch and Ochs, 1992; LeGoascogne and Baulieu, 1977; Padykula et al., 1981], suggests that environmentally induced change in growth conditions or in protein expression is associated with the accumulation of these rather large nuclear structures. Because of the size similarity and the previous suggestions that ND10 are nuclear bodies [Bernstein et al., 1984; Fusconi et al., 1991; Stuurman et al., 1992], we investigated the possibility that nuclear bodies as defined ultrastructurally may contain proteins present in ND10.

Antibodies against ND10 are found in approximately 30% of primary biliary cirrhosis patients [Bernstein et al., 1984; Evans et al., 1991; Szostecki et al., 1992], and the pattern in nuclei is variously described as atypically speckled or

Abbreviations: Ad5, adenovirus 5; EM, electron microscopy; HEp-2 cells, human epithelial carcinoma cells; HRP, horseradish peroxidase; HSV-1, herpes virus type 1; ICP0, intracellular protein 0; IFN, interferon; MAb, monoclonal antibodies; ND10, nuclear domain 10; PBS, phosphate-buffered saline; PCR, polymerase chain reaction; PML, promyelocytic leukemia.

Received May 16, 1995; accepted July 12, 1995.

Address reprint requests to Gerd G. Maul, The Wistar Institute, 3601 Spruce Street, Philadelphia, PA 19104.

nuclear dots. However, sera from patients with other autoimmune diseases [Freundlich et al., 1988], and from a very small percentage of normal volunteer donors [Maul, G.G., unpublished data], also contain antibodies to ND10. These antibodies, and others since developed, are the basis for the immunofluorescence assay that makes it possible to quantitate the frequency of ND10 in single cells.

The first ND10 protein (Sp100) was characterized using primary biliary cirrhosis patients' sera [Szostecki et al., 1990], and its sequence was confirmed by Xie et al. [1993]. No functional information could be derived from the sequence, except that it suggested similarities to RNA binding proteins. A number of monoclonal antibodies (MAbs) react with ND10 and have identified proteins by Western blot analysis with an apparent molecular mass of 65 kDa [Epstein, 1984], 55 kDa [Ascoli and Maul, 1991], and 126 kDa [Stuurman et al., 1992], suggesting that ND10 are multiprotein structures. The potential transactivator promyelocytic leukemia (PML) was found as a partner of the fusion protein with the retinoic acid receptor that results from the t(15;17) chromosome translocation in acute PML [deThé et al., 1991; Goddard et al., 1991; Kakizuka et al., 1991; Kastner et al., 1992; Pandolfi et al., 1991]. The variability of the reported Sp100 size defined by sodium dodecyl sulfate polyacrylamide migration [Szostecki et al., 1990; Xie et al., 1993] and the different splicing variants of PML [Kastner et al., 1992; Pandolfi et al., 1991] suggest that multiple isoforms of these ND10 components exist. This variation, coupled with their low amount, made the identification of these proteins by Western blot analysis difficult, in fact misleading, and the immunofluorescence assay became the investigative tool of choice.

No functions for ND10 have been suggested, although two observations regarding nuclear redistribution of ND10 are indicative of functional changes. First, the antiviral cytokine interferon (IFN), which has antiproliferative activity on normal and transformed cells [DeMaeyer and DeMaeyer-Guignard, 1988], apparently increases the number and size of ND10 by upregulating Sp100 [Guldner et al., 1992]. Second, ND10 structures are targeted by ICP0, an immediate early gene product of herpes simplex virus type-1 (HSV-1). As ICP0 is expressed, it transiently co-localizes with and eventually displaces the host-associated proteins (PML, Sp100, and NDP55) [Everett and Maul, 1994; Maul and Everett, 1994; Maul et al., 1993]. ICP0 is also essential for the stress-induced recurrence of latent HSV-1 [Everett, 1991; Harris et al., 1989]. We, therefore, quantitated the effects of the antiviral cytokine IFN and stress on ND10, and found that heat shock and chemical stress redistribute the ND10 proteins to hundreds of much smaller new sites, whereas IFN treatment increased the number and average size of ND10. Since nuclear bodies represent the ultrastructural equivalent of some ND10, stress IFN and virus-induced changes are the first environmental factors found to modify this nuclear structure.

MATERIALS AND METHODS

Antibodies and Cell Culture

ND10 was visualized using various antibodies. MAb 138 appears to recognize a 55-kDa protein (NDP55) from human epidermoid (HEp-2) cells [Ascoli and Maul, 1991]. MAb 1150, produced against Epstein-Barr virus-infected cell antigens immunoprecipitated from phorbol 12-0-tetradecanoylphorbol-13-acetate-induced Raji cells, recognizes a 65-kDa cellular protein in Western blots with these cells and demonstrates the ND10 pattern in uninduced cells [Epstein, 1984]. MAb 5E10 was generated against a nuclear matrix protein and recognized a 126-kDa protein [Stuurman et al., 1992]. Human autoimmune serum 1745 recognizes ND10 and reacts with Sp100 [Maul et al., 1993; Szostecki et al., 1992]. Isotype-matched MAbs of unrelated specificity were used as controls. Polyclonal rabbit antisera were raised against the 303 N-terminal amino acids of wild-type PML-1 [Kakizuka et al., 1991] and obtained from Dyck et al. [1994]. Rabbit antibodies against Sp100 were from Dr. C. Szostecki. MAbs against the non-snRNP splicing component SC35 were from Fu and Maniatis [1990]. HEp-2 carcinoma cells were maintained in modified Eagle's medium supplemented with 10% fetal calf serum (FCS). All cells were grown at 37°C in a humidified atmosphere containing 5% CO_2. For immunofluorescence, cells were grown on round coverslips in 24-well plates (Corning Glass, Inc., Corning, NY).

To test potential changes in size or frequency of ND10 in response to cytokines, HEp-2 cells were grown in the presence of different cytokines. IFN-β and IFN-γ (1,000 U/ml; obtained from Dr. G. Trinchieri, The Wistar Institute), 5

μm/ml epidermal growth factor (EGF), 10^{-7} μm phorbol 12-0-tetradecanoylphorbol-13-acetate, 5 pg/ml insulin, 5 ng/ml transforming growth factor-β (TGF-β), and 10 ng/ml basic fibroblast growth factor (Collaborative Research, Waltham, MA) were added to the medium for 18 h.

Immunofluorescence Microscopy

HEp-2 cells were fixed at room temperature for 5 min with freshly prepared 1% paraformaldehyde in phosphate-buffered saline (PBS), washed with PBS, and permeabilized for 20 min on ice with 0.2% (v/v) Triton X-100 (Sigma Chemical Company, St. Louis, MO) in PBS. Nuclear antigen localization was determined after incubation of permeabilized cells with human autoimmune serum, rabbit antiserum, or MAb diluted in PBS for 1 h at room temperature. Avidin-fluorescein or avidin-Texas Red was complexed with primary antibodies through biotinylated secondary antibodies (Vector Labs Incorporated, Burlingam, CA). Cells were then stained for DNA with 0.5 mg/ml of bisbenzimide (Hoechst 33258; Sigma) in PBS and mounted with Fluoromount G (Fisher Scientific, Pittsburgh, PA). Fluorescence images were recorded using a Nikon Optiphot or the Leica confocal scanning microscope.

HSV Infection

Wild-type HSV-1, strain 17 syn^+, was used in this study. The mutant strain, D22, was derived from this strain and contains a small deletion close to the RING finger region of the immediate early transcription factor ICP0 [Everett, 1989; Maul and Everett, 1994]. All viruses were propagated and titrated in baby hamster kidney cells grown in modified Eagle's medium supplemented with 10% newborn calf serum. HEp-2 cells were infected with 10 plaque-forming units. Wild-type HSV-infected cells were fixed after 2.5 h p.i., and HSV-1 D22-infected cells were fixed after 5 h p.i. because of the slower progress of infection. Parallel tests with MAb against ICP4 indicated that wild-type-HSV-1 infected 95% and the D22 mutant 85% of the cells.

EM and Ultrastructural Immunohistochemistry

HEp-2 cells uninduced or induced with IFN-β (1,000 U/ml), or infected with HSV-1 wild-type or the HSV-1 mutant D22 [Everett and Maul, 1994] at 10 plaque-forming units per cell or after heat shock, were fixed in 3% glutaraldehyde and processed according to standard procedures [Maul, 1971]. Random cells were scanned at a magnification of ×10,000 and nuclear bodies counted. Using the pre-embedding procedures, antibody reactivity patterns were observed in paraformaldehyde-fixed cells, using immunoperoxidase staining with diaminobenzidine as substrate [Yasuda and Maul, 1990]. After postfixation with glutaraldehyde and osmium tetroxide, cells were sequentially dehydrated in ethanol and embedded in EPON 812. Thin sections were viewed at 60 kV without uranyl acetate enhancement using a Zeiss EM10 transmission electron microscope. The size of structures recognized by antibodies was measured from a series of 30 photographs. For the post-embedding technique, cells were grown in Millicell HA (Millipore, Bedford, MA), fixed in 4% freshly prepared paraformaldehyde, and embedded in LR White Resin (EM Sciences, Ft. Washington, PA). After sectioning and incubation with the primary antibody, the reaction was visualized with 15-nm gold-labeled antimouse or antihuman antibodies (Auroprobe, Amersham Life Sciences, Chicago, IL).

Stress Induction

Exponentially growing HEp-2 cells on round coverslips in 33-mm plastic petri dishes were used 2 days after plating when they reached approximately 80% confluency. Petri dishes were sealed with Parafilm to retain the CO_2 concentration 24 h before the experiment, and floated for different times in a Julabo water bath at 42 ± 0.1°C (chosen as the lowest effective temperature for ND10 after some initial experiments in which temperature was varied). The recovery temperature was 37°C in a CO_2 incubator. Parallel cultures were incubated with or without 100 μg/ml cycloheximide during the stress application or 30 min before stress induction. Stress by exposure to heavy metal was induced by addition of 30 μM $CdSO_4$ to the medium for various time periods.

Production of the Sp100 Plasmid and Transfection

HEp-2 and 3T3 cells were transfected with PML-1 and Sp100 using the DEAE–dextran method, followed by chloroquine and a 1-min incubation in 10% dimethylsulfoxide (DMSO)–Tris. Cells were tested by indirect immunofluorescence 18 h after transfection. The Sp100 gene was isolated by polymerase chain reaction

(PCR) amplification [Sambrook et al., 1989] from a HepG2 cDNA plasmid library [Schild et al., 1990] using the 5′ oligonucleotide 5′ATCAAGCTTCTACCACCACCATGGCAGGTGGGGGCGGCGACCTGA3′ and the 3′ oligonucleotide 5′TCCTGATATCTCTAATCTTCTTTACCTGACCCTCTT3′. These sequences were designed with a *Hin*dIII and an *Eco*RV site in the 5′ and 3′ oligomers, respectively, and are based on the published sequence [Szostecki et al., 1990]. The PCR product was gel-purified, digested with *Hin*dIII and *Eco*RV, and ligated to the pCMX expression vector [Umesono and Evans, 1989], which had been digested with the same restriction enzymes.

GST-Sp100 and GST-PML fusion proteins were generated by PCR from pCMX-Sp100 and pCMX-PML obtained from J. Dyck. The PCR products were digested with *Eco*RI, purified on agarose gels, and cloned into pGEX2TK (Pharmacia, Piscataway, NJ) digested with the same enzyme. Protein expression was induced with 0.1 mM IPTG for 3 h, after which the solubilized fusion protein from the sonicate was bound to glutathione sepharose beads (Pharmacia, Piscataway, NJ).

Aliquots of the proteins bound to beads were solubilized and boiled in denaturing buffer and separated on 8% sodium dodecyl sulfate (SDS) polyacrylamide gels. The proteins were transferred to nitrocellulose membranes (0.2 μg) (Schleicher and Schull), using a semidry transfer apparatus and then probed with various antibodies after blocking with 5% nonfat milk in PBS and 0.1% Tween 20. Secondary antibodies conjugated to horseradish peroxidase (HRP) were used and detected by fluorescence using the ECK kit from Amersham, Inc., Arlington, IL.

RESULTS

Nuclear Distribution of Three Different ND10 Proteins

We have previously shown that ND10-positive sera from patients with primary biliary cirrhosis and three different MAbs stain precisely circumscribed nuclear domains in various vertebrate cell lines [Ascoli and Maul, 1991]. Reactivity of other antibodies led to the conclusion that ND10 are multiprotein complexes [Dyck et al., 1994; Maul and Everett, 1994; Weis et al., 1994]. Among the proteins recognized by MAbs 5E10, 138, and 1150, only PML and Sp100 have been cloned. We therefore tested the different MAb reactivities on these two proteins using HEp-2 cells transfected with plasmids encoding Sp100 or PML to see whether the MAbs react with them, despite the different molecular weights of the proteins with which they had been reported to react [Epstein, 1984; Stuurman et al., 1992]. Rabbit anti-PML and anti-Sp100 antibodies showed the expected reaction, whereas MAb 5E10 reacted with PML-transfected cells (Fig. 1A) but not with Sp100-transfected cells (not shown). After 18 h, the transiently expressed PML localized to sites similar in number but substantially larger than normal ND10. PML was also present diffusely throughout the nucleus and at some cytoplasmic sites. MAb 1150 reacted with Sp100-transfected cells (Fig. 1C), but not with PML-transfected cells (not shown). The overexpressed Sp100 was distributed throughout the nucleus in many specific sites. MAb 138 did not react with either PML- or Sp100-transfected cells. The possibility was considered that the MAb may react with another human nuclear protein induced by either the transfected PML or Sp100. Since both MAb 5E10 and Sp100 do not react with mouse cells [Ascoli and Maul, 1991; Dyck et al., 1994], we transfected 3T3 cells with PML and Sp100. The respective proteins were labeled by MAb 5E10 and MAb 1150, proving that only the transfected protein was recognized.

Western blots of the bacterially expressed Sp100 and PML were evaluated to prove that the respective proteins react with the defined polyclonal antibodies [Ascoli and Maul, 1991; Dyck et al., 1994; Szostecki et al., 1992] and to test whether the ND10-specific MAbs react as found by labeling transiently expressed proteins. In addition, we tested two human autoantibodies used in various double labeling procedures [Ascoli and Maul, 1991; Maul and Everett, 1994]. The same set of antibodies are used in the left panel of Figure 2 with GST-PML, and in the right panel with GST-Sp100. The rabbit anti-Sp100 and PML recognize their respective proteins only. GST alone did not react with the antibodies (not shown). The low-molecular-weight bands labeled by the rabbit anti-Sp100 in the PML panel are carried over *Escherichia coli* crossreactive bands. Both rabbit antibodies recognize several proteolytic fragments. MAb 1150 and 5E10 react only with one full-length fusion protein, proving that MAb 1150 is specific for Sp100 and MAb 5E10 for PML. The failure to obtain acceptable Western blots from total cell extracts may be due to high susceptibility to proteolysis of Sp100 and PML. The human auto-

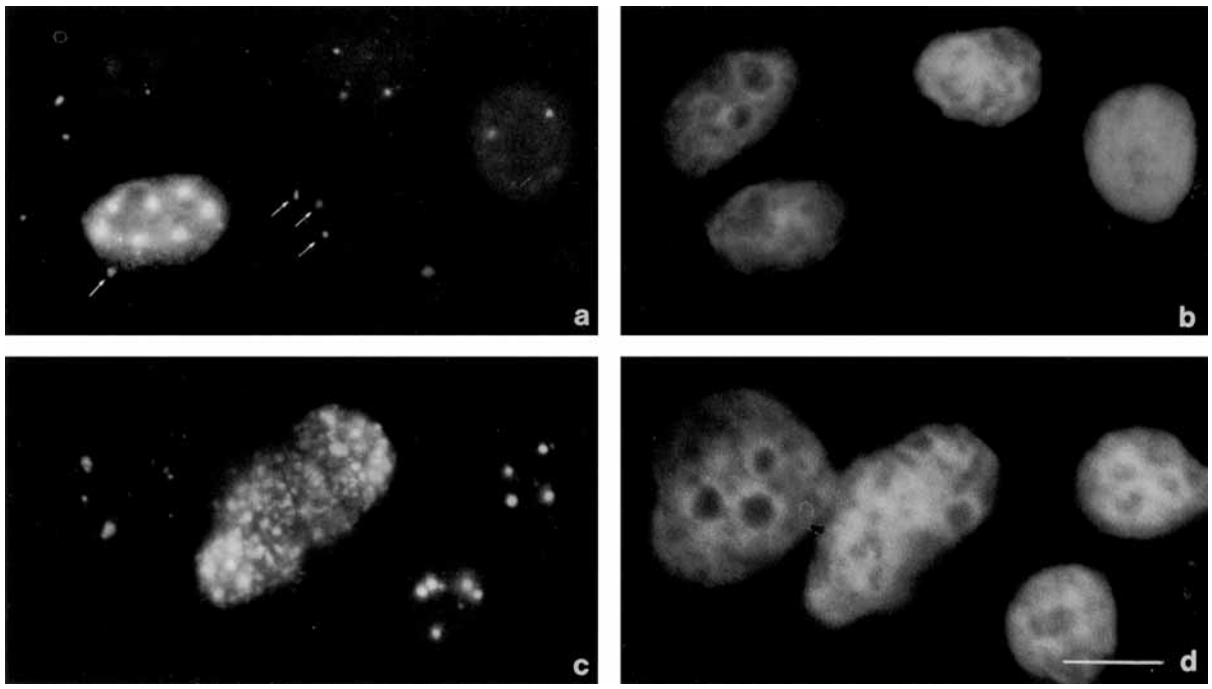

Fig. 1. **A:** PML-transfected HEp-2 cells stained with MAb 5E10, showing an increased size of a few antigen-positive sites and diffuse nuclear staining. *Arrows,* cytoplasmic antigen-positive sites. **C:** In Sp100-transfected cells stained with MAb 1150, the nucleus appears to be filled with many small antigen-positive sites. Both images were taken 18 h after transfection, and are representative for the respective proteins. **B,D:** Same cells as in **A** and **C**, respectively, stained for DNA to compare positive and negative cells. Bar = 10 μm.

antibody 1157 labeled Sp100. However, the human autoantibody 1745 reacted with both proteins, a quite unexpected finding. We found that about 30% of sera recognizing ND10 are also reacting with PML (data not shown).

The three MAbs representing PML, Sp100, and NDP55 most obviously stain ND10 and co-localize with rabbit antibodies to PML and Sp100 [Ascoli and Maul, 1991; Dyck et al., 1994]. However, subtle differences in the staining of the nucleoplasm were observed. All nuclear staining of Sp100 (Fig. 3A) is confined to ND10. The postmitotic cell pair (Fig. 3A, arrows) has only faint positive dots. In addition to ND10, NDP55 shows a distinct grainy nuclear staining pattern, which is enhanced in the postmitotic cell pair (Fig. 3C, arrows). PML exhibits the greatest variation in nuclear staining intensity between cells (Fig. 3E,F). In addition, PML is present in cytoplasmic aggregations, most frequently observed in cell pairs, which may be in early G_1-phase (Fig. 3F). Comparison of ND10-associated proteins demonstrates that PML and NDP55 are present throughout the nucleus, except in the nucleolus of the continuously dividing HEp-2 cell.

Effect of IFN on ND10 Frequency and ND10 Protein Distribution

The effect of the antiviral cytokine, IFN, which increases ND10 frequency [Guldner et al., 1992], was quantitated, and the changes in intranuclear distribution of ND10-associated proteins were determined with the three MAbs (1150, 5E10, and 138) after 18 h IFN-β and IFN-γ treatment (1,000 U/ml). The nuclei of treated HEp-2 cells are larger (Fig. 3B,D,F) than those of the untreated controls (Fig. 3A,C,E). The staining of ND10 is increased, the number elevated, and their size is more homogeneous; i.e., there are fewer smaller ones. No change in nucleoplasmic staining was found for Sp100. NDP55 is diminished throughout the nucleus relative to the untreated control. Even the postmitotic cell pair in Figure 3D (arrows) shows no staining in the nucleoplasm. In contrast, diffuse PML staining of the nucleoplasm is considerably enhanced after IFN treatment and, in some cells, obscures staining of ND10 (Fig. 3F). Thus analysis of the staining patterns of the three MAbs after IFN treatment shows that the frequency of ND10, as well as the intensity of the

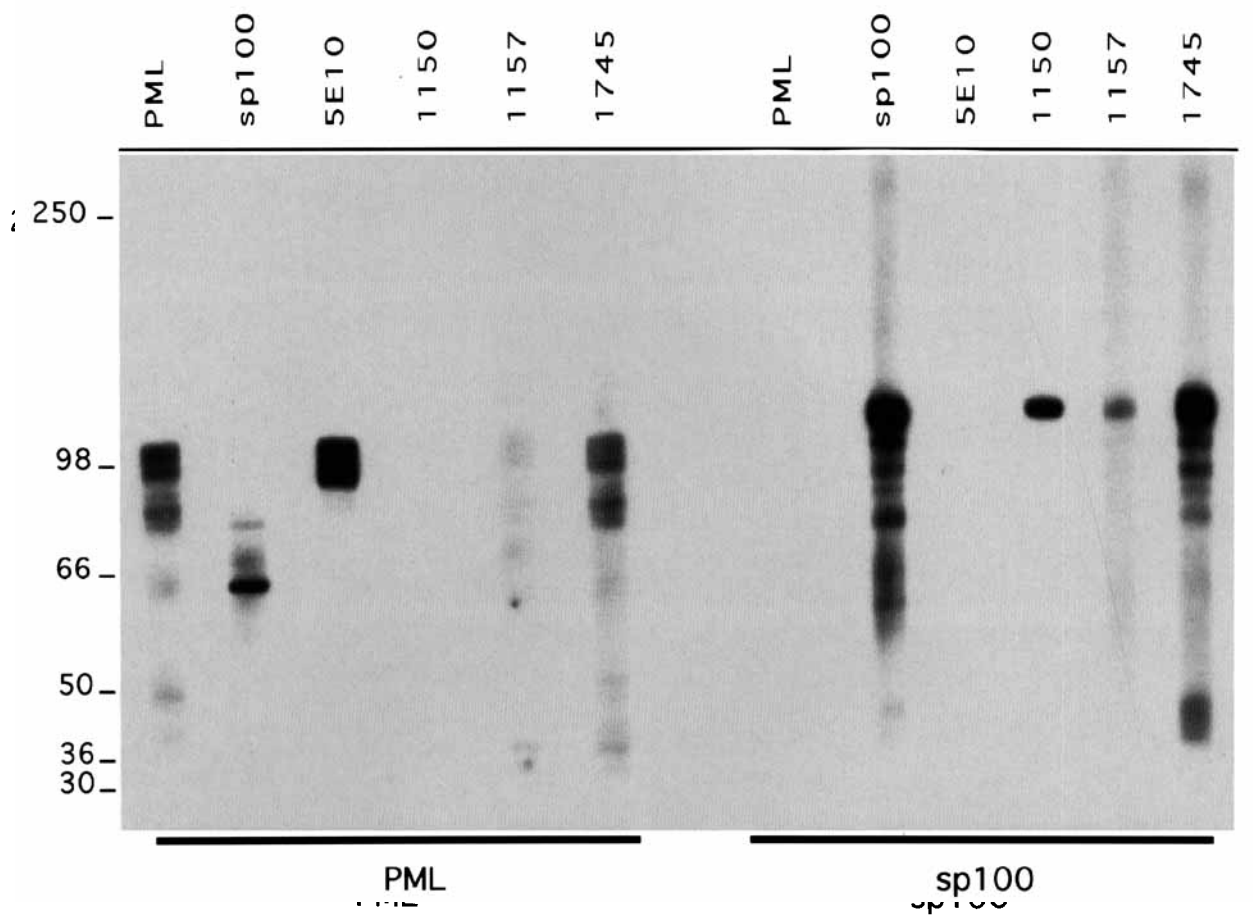

Fig. 2. Western blot data of bacterially expressed Sp100 and PML. Separate strips of both proteins were reacted with the respective antibodies designated at the top.

diffuse nuclear staining for PML, are increased, whereas NDP55 labeling is decreased throughout the nucleus, suggesting that the three different proteins are differentially influenced by this cytokine. In exponentially growing HEp-2 cells approximately 80% confluent, we found that ND10 doubled in frequency after IFN treatment (Table I). There was no significant difference between treatment with IFN-β and IFN-γ. Also, all antibodies tested showed this doubling. No significant change was induced with other cytokines tested (insulin, EGF, transforming growth factor-β (TGF-β), basis fibroblast growth factor, phorbol 12-0-tetradecanoylphorbol-13-acetate) (not shown). The substantial increase in ND10 number can be used to correlate changes at the ultrastructural level.

ND10 Redistribution of Associated Proteins After Heat Shock

ND10 are eliminated shortly after HSV-1 infection [Maul et al., 1993]. Mutants of the immediate early transactivator, ICP0, do not induce this change [Maul and Everett, 1994]. Since ICP0 is essential for the recurrence of HSV-1 after stress, we analyzed the effect of stress in the form of heat shock on ND10. Hyperthermia typical of high fever (42°C for 60 min) induced the dispersion of ND10 (Fig. 4, cf. A and B) into hundreds of microdots throughout the nucleus with all ND10-specific antibodies. No such major redistribution of the control splicing factor SC35 occurred, although the splicing domains became more precisely circumscribed and lost their anastomosing connections (data not shown; see also Spector et al. [1991]).

We characterized this heat-induced phenomenon in HEp-2 cells at temperature intervals of 0.5°C from 37°C to 45°C for 60 min. Sp100 redistribution from a few to many sites occurred at 41.5°C to 42°C (Fig. 4B). At 45°C, most of the cells retained only a few Sp100 sites with weak reactivity (Fig. 4C). The cell pair at the left has lost nearly all of the small sites, while the right pair has retained a few. The redistribution response clearly occurs in the range of high fever

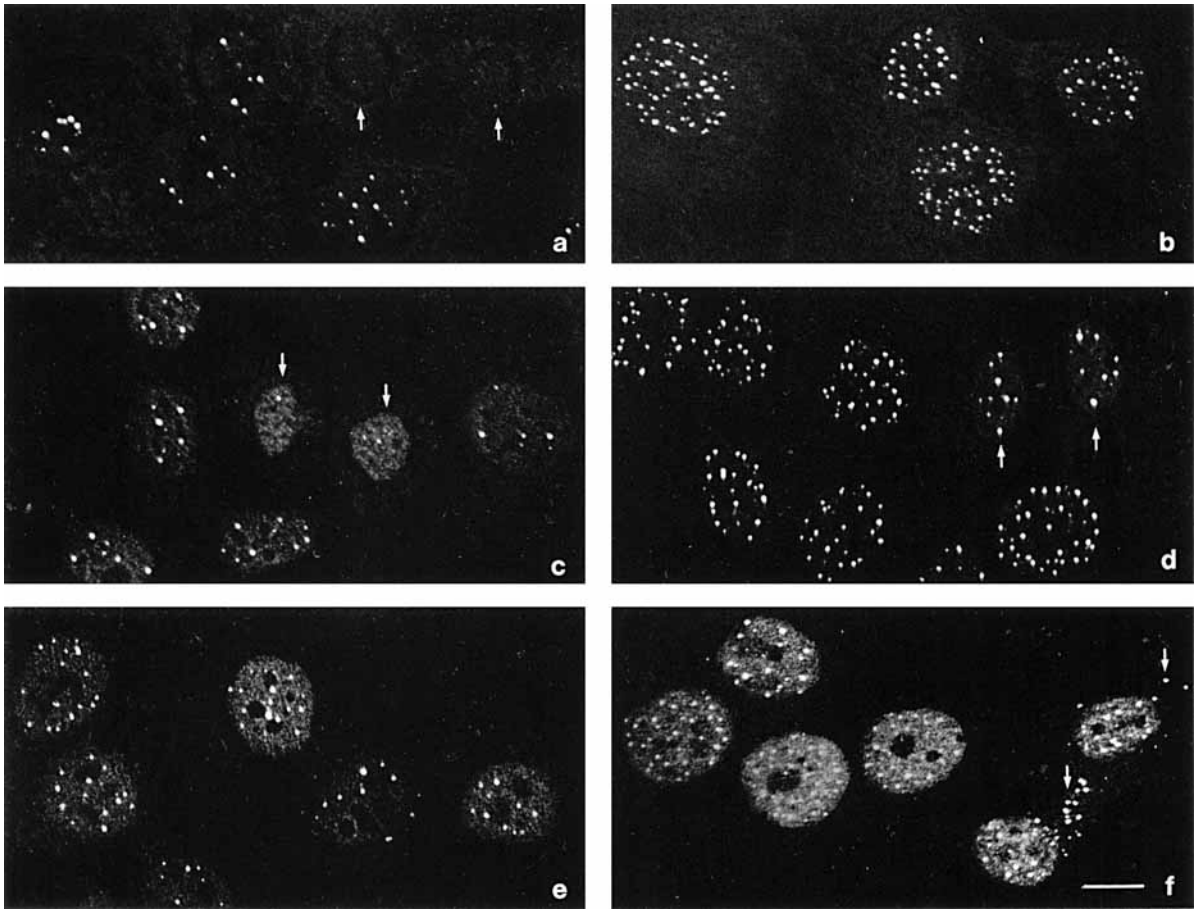

Fig. 3. Antigen distribution and ND10 frequency as a function of growth conditions. **A:** Exponentially growing HEp-2 cells stained with MAb 1150 showing the brightly stained ND10 and unstained chromatin. *Arrows,* point to a postmitotic cell pair. **B:** MAb 1150-stained HEp-2 cells after 16-h IFN-β treatment have larger nuclei and more ND10. **C:** HEp-2 cells reacted with MAb 138 show ND10 and a fine granular nuclear staining excluding nucleoli. This reaction is particularly evident in the postmitotic cell pair (*arrows*). **D:** After IFN-β treatment, nuclear background staining is decreased, with the decrease in MAb 138 staining particularly evident in the postmitotic cell pair (*arrows*). **E:** HEp-2 cells reacted with MAb 5E10 show ND10 and a variably strong fine granular nuclear staining excluding nucleoli. **F:** HEp-2 cells after IFN-β treatment and incubation with 5E10 show coarse nuclear staining in all cells, and pairs of cells with equal nuclear size show a similar frequency of ND10 and nuclear staining intensity. One cell pair has cytoplasmic granules (*arrows*). **A–F:** Same magnification indicated in **F.** All bars = 10 μm.

TABLE I. IFN Modulation of ND10 Frequency in HEp-2 Cells*

Antibodies	Control	IFN-β	IFN-γ
MAb 1150; Sp100	10.2 ± 3.9	23.7 ± 8.4	21.5 ± 7.7
MAb 5E10; PML	9.9 ± 3.4	23.0 ± 7.5	23.5 ± 6.4
MAb 138; NDP55	9.6 ± 2.3	22.5 ± 6.2	19.6 ± 4.9

*Fifty exponentially growing cells in each treatment group were scored for ND10 frequency, using the three MAbs that detect the indicated proteins.

(42°C), and the antigen is apparently lost at lethal temperatures (45°C). Thus, we selected 42°C for further time course experiments.

No redistribution to microdots was seen after 5 min. However, after 10 min, a few cells (often in pairs) demonstrated this redistribution. Concomitant with the appearance of the microdot pattern, the number of ND10 diminished (Fig. 4D). The apparent large size of the ND10 relative to the control is due to the light dispersion during the procedure used to photographically reproduce the microdots. When the 10-min heat treatment was followed by a 10-min recovery at 37°C, the number of antigenic sites increased dramatically in all cells, indicating that while a 10-min treatment is enough to trigger the response, further time is required for the response to develop. After a 20- or 30-min heat shock, the response became stronger and, by 60 min, differ-

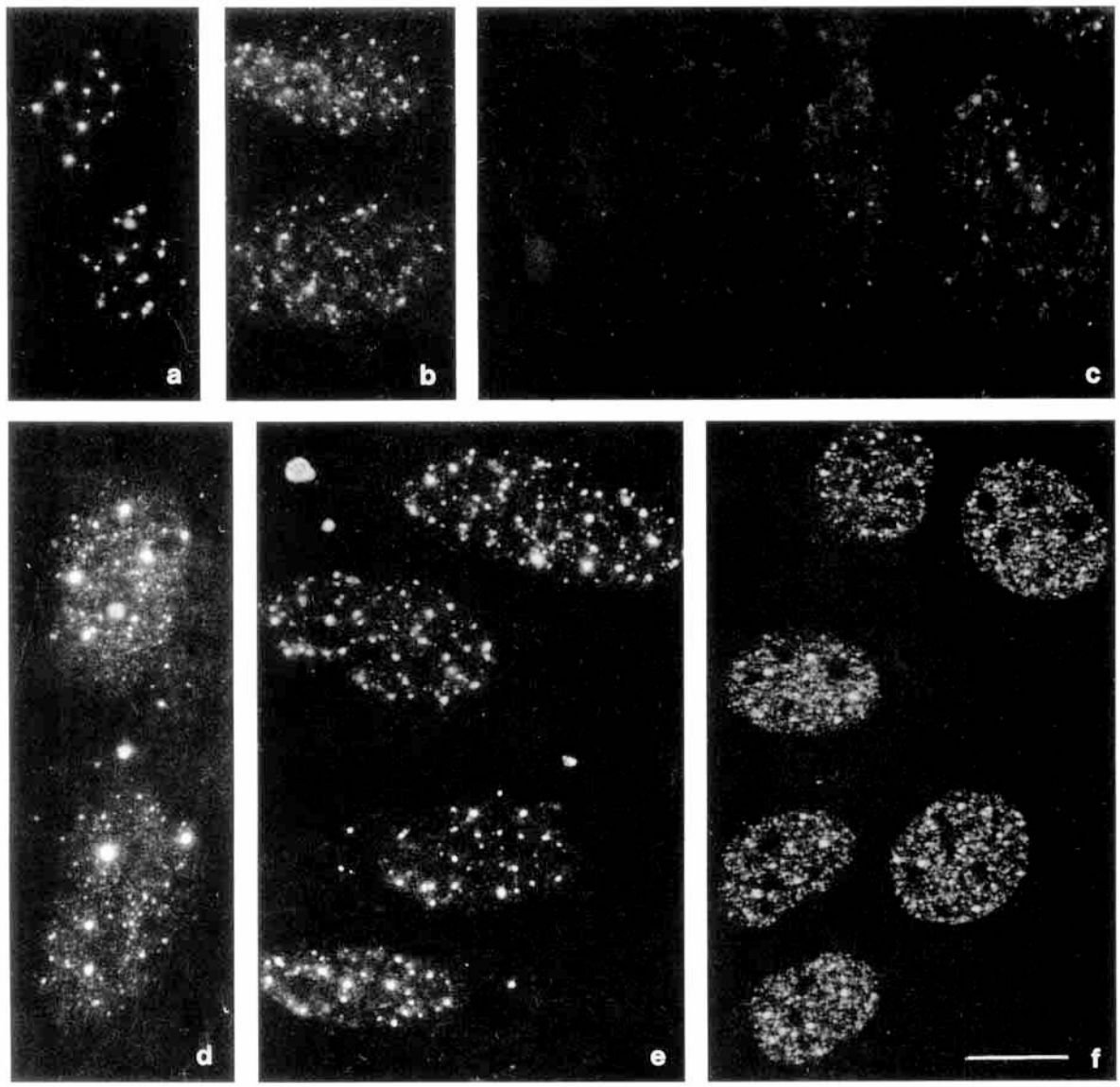

Fig. 4. Heat shock-induced redistribution of ND10 antigens. Different HEp-2 cell cultures were incubated at temperature intervals of 0.5°C for 1 h. **A:** Control at 37°C reacted with MAb 1150. **B:** Cells incubated at 42°C and reacted with MAb 1150 show a large number of small dots, most of which appear faint. **C:** Cells incubated at 45°C using MAb 1150. Of the two cell pairs shown, the left pair has almost no small dots, the right pair retains a few. **D:** Cells incubated at 42°C show changed distribution of reactivity with MAb 5E10 after only 10 min. The few large dots are exaggerated through long exposure to visualize the small dots. The large dot outside the nucleus represents PML in the cytoplasm. **E:** Two cell pairs reacted with MAb 5E10 after 42°C for 60 min. Again the cells are overexposed to show the large number of small dots. The larger ND10 are diminished in staining intensity. **F:** MAb 138 used after 60 min of heat shock at 42°C reveals the strongly enhanced sandy appearance throughout the nucleus except the nucleoli. This image was obtained with the confocal microscope as a single optical section. Bar = 10 μm.

ences between Sp100, PML, and NDP55 became apparent (Fig. 4B,E,F). Sp100 staining was diminished; i.e., the sites became smaller and dimmer, and there was more diffuse staining of the nucleus (Fig. 4B), whereas PML retained the brilliant, precisely localized microdot staining (Fig. 4E). Most dramatic was the increased NDP55 staining (Fig. 4F), which covers all areas of the nucleus except the nucleolus and is substantially more intense than that of PML. These observations further demonstrate the differential behavior of each of the three ND10-associated proteins.

To analyze the potential reversibility of the heat shock response, we utilized a 1-h heat shock at 42°C, and observed cells at different times of

recovery up to 16 h at 37°C (Table II). This quantitative evaluation shows that a steady recovery occurs over an extended period, indicating the variability between cells. At 30 min, only a very few cells showed recovered ND10 (antigen-positive domains of increased size). At 4 h, recovery was well advanced and by 8 h, complete. No mitotic figures were found before 8 h, demonstrating that cell division with its concomitant reconstruction of the nucleus is not essential for ND10 reassembly. In fact, a mild synchronizing effect was observed with a higher than expected mitotic index at 16 h. Thus, response to heat shock is rapid (10 min) compared to ND10 reassembly, which requires 4–8 h.

To determine whether this response to heat shock was inducible by other types of stress, we analyzed the effect of $CdSO_4$ treatment. No changes were seen after 30 min but, by 60 min, a strong redistribution was recognized similar to that induced by 42°C for 20 min. At 2 or 3 h, there was less staining, but Sp100 did not disappear (data not shown). Thus, our observations on heat shock generalize at least to $CdSO_4$-induced stress.

To determine whether the increase in nuclear antigen-positive sites is a result of the classical heat shock response (i.e., heat shock factor activation followed by heat shock protein synthesis), heat shock protein synthesis was blocked with 100 μg/ml cycloheximide either during or beginning 30 min before application of a 30-min heat shock. We observed no change relative to controls (not shown), indicating that heat shock protein synthesis is not necessary for the redistribution of ND10 proteins. Glycerol prevents activation of the heat shock factor [Edington et al., 1989], probably through the protection of thermolabile proteins. When 1 M glycerol was applied 30 min before a 1-h heat shock at 42°C, no inhibition of ND10 protein redistribution was detected (not shown), indicating that the redistribution is probably independent of heat shock factor activity or, for that matter, protein denaturation. Heat shock at 40°C can adapt the cell by activating the heat shock factor and heat shock protein synthesis [Li and Werb, 1982; Milkman, 1966; Mitchell et al., 1979]. This activation itself did not result in ND10 redistribution. If the redistribution of ND10 proteins could be prevented by the presence of newly synthesized heat shock proteins, no redistribution would be expected upon challenge with 42°C. In fact, HEp-2 cells incubated at 40°C for 1 h, conditions in which distribution of ND10 remained at control levels, and at 37°C for an additional 5 h to allow for heat shock protein synthesis before challenge with a 60-min 42°C heat shock, showed the usual microdot distribution of antigens (data not shown), suggesting the absence of any detectable adaptation, and thus independence of heat shock protein synthesis. In conclusion, the experiments above strongly suggest that the change observed in ND10 protein distribution is independent of the classic heat shock response.

Search for the Ultrastructural Equivalent of ND10

The change in number of ND10 upon IFN treatment allowed an ultrastructural search for structures that increased in frequency and that might therefore be the ND10 equivalent. We looked for compact structures in face-on sections of nuclei that resembled the precisely circumscribed immunofluorescent images. Figure 5A (lower left) shows two loose nuclear bodies, and the upper left shows two dense nuclear bodies of the appropriate size and shape. Based on the increase in ND10 frequency by IFN, and

TABLE II. ND10 Reemergence After Heat Shock*

	Hour after recovery						
	0	0.5	1	2	4	8	16
% cells with ND10	100	4.0	17	30	68	100	100
No. of ND10	10.3 ± 3.4	—	16.3 ± 48	12.5 ± 3.3	11.8 ± 3.5	13.9 ± 4.6	12.2 ± 3.0
P-value	—	—	—	< 0.001	0.29	0.009	0.05
% of mitotic cells	1.9	0.0	0.0	0.0	0.0	2.7	7.1

*HEp-2 cells were heat-shocked for 1 h at 42°C and allowed to recover for different times at 37°C. Average values were from recovered cells, i.e., only those that showed ND10. The percentage of cells with ND10 increased with time of recovery. Mitotic cells are not included in cells with ND10. Significance was determined between time points by Student's *t*-test. The significant difference between 4 and 8 h might reflect the larger percentage of cells in the latter part of the cell cycle as recognized by larger nuclei. Between 30 and 40 cells were counted for each time point.

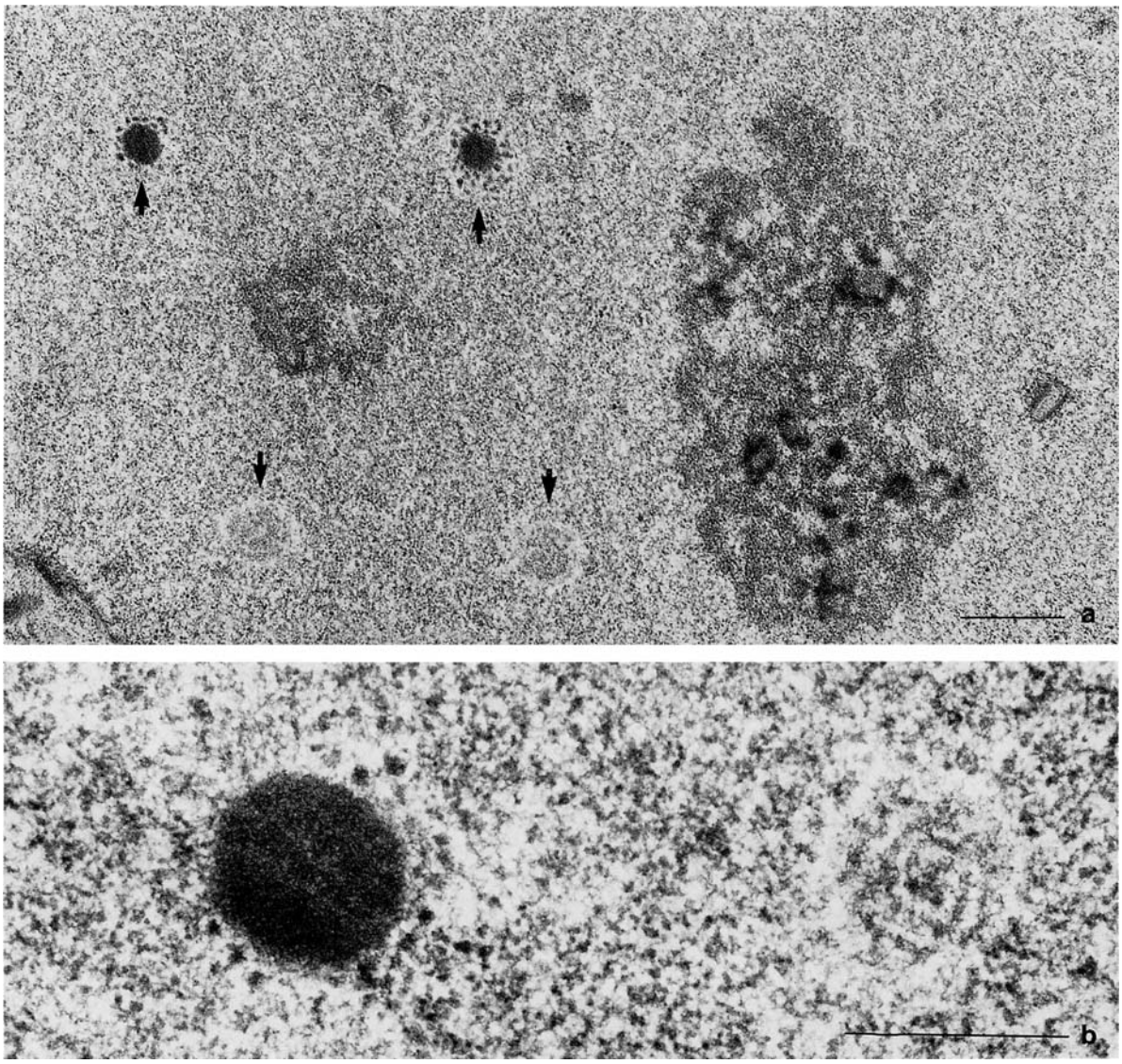

Fig. 5. Electron micrographs of HEp-2 cells after 18 h of IFN-γ treatment. **A:** The survey figure demonstrates the presence of two dense nuclear bodies (*upper arrows*) and two loose nuclear bodies (*lower arrows*). Bar = 1 μm. **B:** Dense nuclear bodies with dense fibrillar material and loose nuclear bodies, excluding chromatin. Fine fibers connect the loose nuclear bodies to chromatin. Bar = 0.5 μm.

our observations that heat shock redistributes ND10 antigens to many sites and that HSV-1 eliminates ND10 staining [Maul et al., 1993], we analyzed the EM-visible nuclear structures for corresponding changes. As summarized in Table III, the dense variety of nuclear bodies did not vary in number with IFN-β treatment. The loose and fibrillar form, however, was seen substantially more often after IFN-β stimulation and was also removed by wild-type HSV-1 infection. The dense nuclear bodies were not counted in the wild-type virus-infected cells, since there was no difference between the structure of the dense nuclear bodies and the segregating remnants of nucleolar fibrillar centers resulting from nucleolar breakdown. As previously shown, the D22 HSV-1 ICP0 mutant lacking an active RING finger motif does not eliminate ND10 early during infection [Maul and Everett, 1994]. Thus, this mutant served as a control showing that infection by itself did not result in the elimination of nuclear bodies. After heat shock treatment no loose bodies were found. The results of this semiquantitative analysis indicate that the loose nuclear bodies increase in number upon IFN treatment and are eliminated by HSV-1

early during infection and by heat shock; i.e., the loose nuclear bodies react like ND10 to environmental influences.

However, comparison of the ND10 and nuclear body frequencies showed a substantial discrepancy. The number of ND10 expected at the ultrastructural level was, therefore, determined experimentally from direct observation of nuclei stained for NDP55 and peroxidase-labeled second antibodies in a pre-embedding procedure counting 34 nuclear sections (see Fig. 6A). At the light microscopy level, HEp-2 cells have the same number of ND10, whether reacted with fluorescein-labeled second antibodies or peroxidase-labeled second antibodies. Therefore, the average number seen by EM, for which the same peroxidase technique is used, should give the same number. We found 2.2 antigen-positive sites versus 0.48 dense nuclear bodies and only 0.29 loose nuclear bodies per section in glutaraldehyde-fixed cells. Calculation of the total nuclear bodies (see footnote to Table II) and comparison to ND10 indicates that ND10 are 2.8-fold more abundant than total nuclear bodies and 6.7-fold more prevalent than loose nuclear bodies. We interpret this discrepancy as an incomplete correspondence of ND10 to nuclear bodies.

The loose nuclear bodies are surrounded by a halo consisting of fine fibrils that connect the bodies to the rest of the nucleus (Fig. 5B, right). The loose and dense nuclear bodies are approximately 0.5 μm in diameter (Fig. 5B). The dense nuclear bodies do not have a recognizable substructure, but are often partially surrounded by thick strands (Fig. 5A,B). Using pre-embedding immunohistochemical techniques, the images obtained (Fig. 6A) differ from those of nuclear bodies in glutaraldehyde-fixed cells. Most positive areas contain reaction products on fibers the size of chromatin, and the reaction product ends abruptly within a single fiber (Fig. 6B, arrow). Several ring-like structures were resolved (Fig. 6C,D), as expected from some of the immunofluorescence images. These structures might represent the dense bodies, which because of their dense core might exclude antibodies, or might lack the antigen inside.

We used immunogold labeling in a post-embedding procedure to increase the structural integrity of the nucleus for identification of Sp100 and PML. However, the addition of even small amounts of glutaraldehyde reduced specificity to undetectable levels with all our antibodies. The immunogold technique using paraformaldehyde-fixed cells revealed a ring-like outline of the antigen in some large nuclear bodies (here shown for Sp100 and PML using the human autoantibody 1745; Fig. 7A–C), although totally labeled nuclear bodies were also found (Fig. 7D). The recognition of some of the underlying structures obtained with the post-embedding technique suggested that some of the dense nuclear bodies contain Sp100 and PML around their

TABLE III. Estimation of Nuclear Bodies in HEp-2 Cells*

	Dense nuclear bodies			Loose nuclear bodies		HRP-reactive sites	
	Sections analyzed	Observations per section	Total per nucleus	Observations per section	Total per nucleus	Observations per section	Total per nucleus
Control	31	0.48	2.40	0.29	1.45		
IFN-β	41	0.41	2.05	1.97	9.85		
Wild-type HSV	29	—	—	0.03	0.15		
IFN-β wild-type HSV	42	—	—	0.02	0.10		
IFN-β HSV-D22	33	0.48	2.40	1.27	6.35		
1 h heat shock	41	0.61	3.05	0	0		
Control HRP EM	34					2.2	11.00

*Two types of nuclear bodies, dense or loose (see Fig. 5), were counted by EM in face-on nuclear sections. A nuclear height of 2.5 μm was used for calculation of nuclear bodies per nucleus. A section thickness of 80 nm (silver interference color) gave 31 sections per nucleus. Thus, approximately one nuclear equivalent of sections was analyzed. Since the height of the average nucleus and of the average nuclear body is 2.5 μm and 0.5 μm, respectively, the probability of observing randomly distributed nuclear bodies in a noninfinitely thin section is at least 1/5. Therefore, the mean value of observation per sectioned nucleus multiplied by five gives the estimated total number of nuclear bodies per nucleus. The actual number observed is listed under sections analyzed and then multiplied by five to show the estimated nuclear body frequency per nucleus. The results indicate that IFN-β induces the formation of loose nuclear bodies and wild-type HSV-1 eliminates them even if previously induced by IFN-β. Cells reacted with MAb 138 and HRP were treated the same as the glutaraldehyde-fixed cells, and the reaction product-positive sites counted. The number of ND10 determined by immunofluorescence (see Table I) corresponds with that of the HRP reaction product-positive sites; i.e., they are most likely the equivalent of ND10.

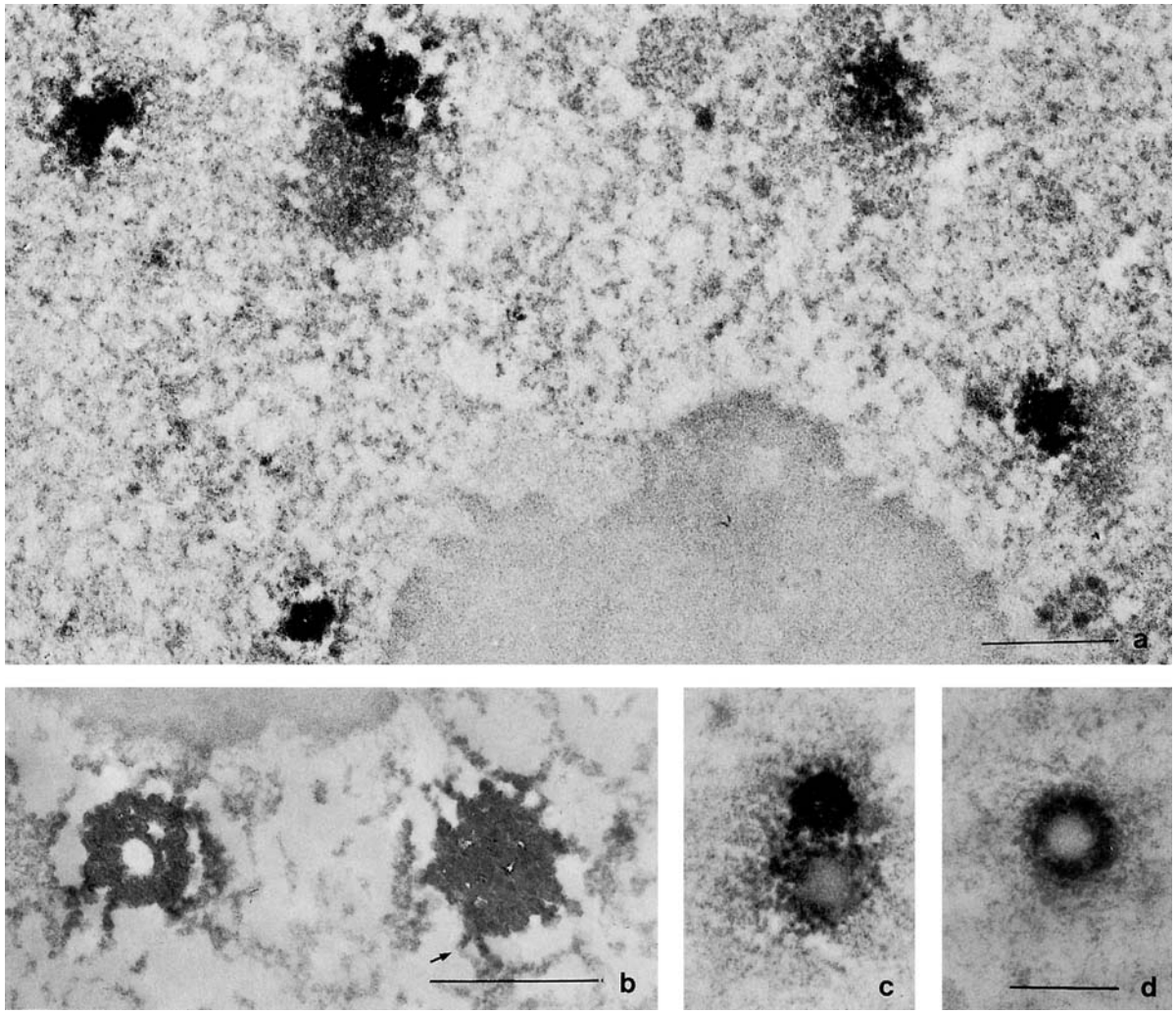

Fig. 6. HEp-2 cells reacted with autoantibody 1745 in a pre-embedding procedure using peroxidase-labeled second antibodies. **A:** The survey figure demonstrates the general outline of staining. Bar = 1 μm. **B:** ND10 are mostly stained throughout with emanating fibers that have the size of chromatin. *Arrow,* cessation of visible reaction product. Bar = 0.5 μm. **C,D:** Antigen-positive ring structures. Bar = *D represents* 1 μm; same magnification in **C.**

periphery. Gold grain accumulations over undistinguished chromatin areas or areas apparently devoid of structure may label ND10 and the loose nuclear bodies. ND10, as defined by immunofluorescence, then consists of domains not visible by EM, of dense nuclear bodies, and probably (as determined by the same responses to IFN, stress, and HSV-1 infection) of loose nuclear bodies.

DISCUSSION

Some ND10-Associated Proteins are Present Throughout the Chromatin and on Nuclear Bodies

We previously suggested that ND10 represent new nuclear domains [Ascoli and Maul, 1991], based on co-localization attempts with various known domains. The similarity in size (0.3–1.0 μm), the precise circumscription of the light microscopic image, and a frequency increase of ND10 in estradiol-treated rat uterus lining has led to the suggestion that NDs recognized by sera of primary biliary cirrhosis patients are nuclear bodies [Bernstein, 1984; Fusconi et al., 1991], which are interchromatinic structures described much earlier [deThé et al., 1960]. The question of whether ND10 and nuclear bodies are identical must be resolved, since ND10 (also called PML oncogenic domain) [Dyck et al., 1994] are altered in APL, although no ND10 can be seen in leukemia cells. Instead, PML and the PML-retinoic acid receptor fusion proteins are

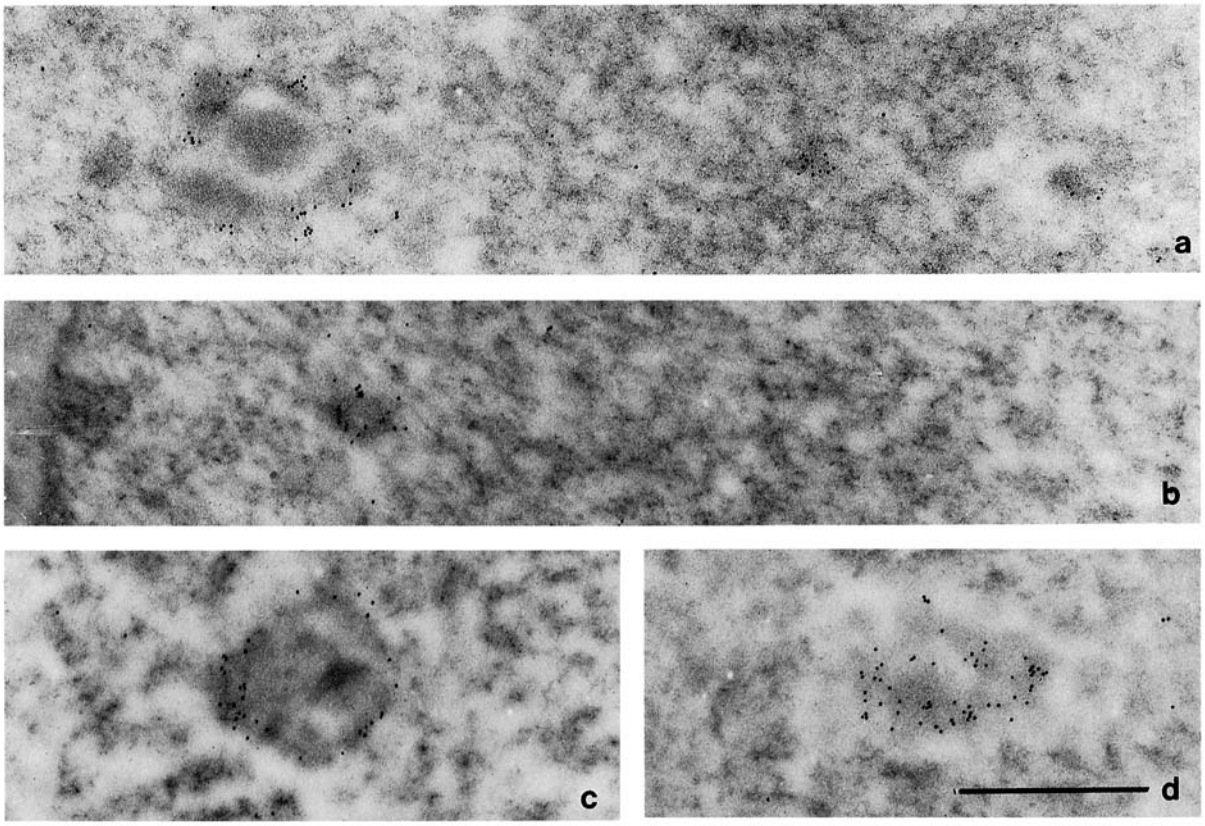

Fig. 7. Post-embedding immunogold labeling of paraformaldehyde-fixed, IFN-γ-stimulated HEp-2 cells using human autoantibody 1745. **A:** A large nuclear body has gold particles arranged in a ring at the outer perimeter. A smaller cluster of gold particles is present over a nuclear area without structural distinction. Another smaller nuclear body has a few gold particles localized over it. **B,C:** Various-sized large nuclear bodies have gold particles in their outer perimeter. **D:** Total labeling of a large nuclear body. Bar = 1 μm.

distributed in hundreds of very small sites that give the nucleus a grainy appearance in immunofluorescence images [Dyck et al., 1994; Weis et al., 1994]. These images are similar to those after heat shock. Upon all-trans retinoic acid treatment, NB4 cells demonstrate aggregation of PML into the larger ND10, and this change accompanies the differentiation of a promyelocyte to a nondividing granulocyte. Thus, potential functions of PML in ND10 or nuclear bodies might be important for differentiation.

Our finding of an interaction of an immediate early viral protein with ND10 raises the question of whether nuclear bodies are essential for the successful and efficient replication of HSV-1. ICP0 is essential for the stress-induced reactivation of HSV-1 from latency. The viral protein augments transcription [Everett, 1988], contains the same RING finger motif as PML, and can eliminate ND10 [Maul et al., 1993]. We found that the RING finger region is necessary for this change [Everett and Maul, 1994; Maul and Everett, 1994], although it remains unclear whether elimination of PML from ND10 is affected by the viral transactivating protein through direct interaction. ICP0 binds transitionally to this structure, and remains bound to ND10 in the continued presence of PML if the RING finger region is mutationally inactivated. Under these circumstances, PML, Sp100, and NDP55 redistribute to many microdots as in heat shock or to long nuclear tracks that are apparently virus induced. The viral ICP0 may circumvent ND10-associated protein function.

The target site of PML function needs to be determined, since the strategies for isolation of functional complexes will be quite different depending on whether the functional activity is in the compact nuclear bodies or spread throughout the chromatin. Our semiquantitative results indicate that not all ND10 are nuclear bodies. The 7-fold increase in detectable loose nuclear bodies does not correlate with the IFN-induced doubling of ND10 number. Both ND10

and loose nuclear bodies increase in frequency upon IFN treatment and are eliminated by HSV-1 infection and heat shock. Thus, both structures could be seen in immunofluorescence as ND10. Alternatively, the EM-recognizable structures may come about through additional assembly of IFN-induced proteins on pre-existing ND10, making them visible ultrastructurally; i.e., new loose nuclear bodies may form on pre-existing ND10, an interpretation presently favored. By contrast, dense nuclear bodies do not decrease in number after heat shock or increase after IFN treatment, although they also contain Sp100 and PML on their periphery, as revealed by specific immunogold labeling, and therefore would appear as ND10 in immunofluorescent images.

The antigens recognizing ND10 have subtle but significant differences in their distribution. NDP55 and PML are not only present in ND10, but are also distributed throughout the chromatin in a grainy fashion in HEp-2 cells. On the other hand, Sp100 appears to be present only in ND10. Aside from its presence in ND10, PML is selectively increased throughout the nucleus after IFN treatment. The presence of NDP55 after heat shock in the nucleoplasm is substantially enhanced. These observations suggest that major changes in the cell environment can trigger redistribution of ND10-associated proteins throughout the nucleus.

The search for the functional site of PML might reasonably begin at the locus of its highest concentration. When these loci appear to correspond to ultrastructural features long recognized but of unknown significance [deThé et al., 1960], and when the protein found in them is derived from a potential oncogene [Dyck et al., 1994], ND10 may be investigated to the exclusion of other possible sites of PML function. Such an investigation may prove unprofitable if the highly concentrated accumulations of PML, Sp100, and NDP55 represent inactive storage sites. We hypothesize that the antiviral IFN signals the cell to accumulate specific proteins preemptively. The cell then stores these proteins, which are poised for immediate redistribution upon stress emergencies such as heat shock, chemical stress, or viral infection.

Heat Shock Redistributes PML from ND10 to Many Specific Sites Throughout the Chromatin

A short, mild heat shock (42°C for 10 min) redistributes the ND10 proteins throughout the nucleus in a manner independent of protein synthesis. This redistribution is accompanied by the elimination of the loose nuclear bodies, but not the dense ones. Experimental conditions that reportedly block heat shock factor activation, i.e., glycerol [Edington et al., 1989], do not block redistribution. We also did not detect the adaptive behavior characteristic of the heat shock response [Li and Werb, 1982; Milkman, 1966; Mitchell et al., 1979]. Therefore, the observed phenomenon is probably not dependent on heat shock factor-induced transcription and synthesis of heat shock proteins. Also, the redistribution is very fast and complete before substantial heat shock protein synthesis is possible.

Both heat shock and IFN treatment slow cell cycle progression, but induce very different effects on the distribution of PML and the other ND10-associated proteins. IFN production by cells is induced in response to viral and other infections [DeMaeyer and DeMaeyer-Guignard, 1988; Isaacs and Lindenmann, 1957], and acts on neighboring cells by activating a limited number of proteins including double-stranded RNA protein kinase, which reduces translation of capped mRNA [Lengyel, 1993; Merrick, 1992]. If PML and the other ND10 proteins are part of the IFN-induced cellular defense mechanism, one might expect them to be translated, accumulated, segregated, and appropriately deployed only upon infection. The increase in nuclear bodies then might enable ND10 ultrastructural recognition through specific preemptive protein accumulation. One may also expect that these proteins are involved in the defense against virus-induced functions. However, PML associates with HSV-induced nuclear structures only in the absence of functional ICP0 [Maul and Everett, 1994; Maul et al., 1993]. An ND10 function detrimental to HSV-1 may exist for which this particular virus has evolved a countermeasure in the deployment of ICP0 (see references in Garfinkel and Katz [1993], for review). We recently showed that adenovirus 5 also modifies ND10 by placing all its proteins into track-like structures. Here, the separation into a different structure may serve the same purpose of neutralizing suppressive function (in preparation). Other viruses need to be investigated to determine whether these changes have more general relevance.

Our results do not explain the mechanism by which ND10 proteins function and only suggest that they act at multiple sites throughout the

nucleus. Both stress and infection are environmental threats to the cell and may require defensive action. The slowing of cell cycle progression by stress results not only from protein denaturation but also from the inhibition of splicing of new pre-mRNA. Heat shock does reduce splicing despite continuing transcription [Bond, 1988; Utans et al., 1992; Yost and Lindquist, 1986]. It also results in a strong influx of proteins that may alter nuclear structure by changing the balance of proteins. Common to any change in ND10 or nuclear body frequency are major changes in nuclear function like those induced by heat shock, hormone-activated differentiation, or viral replication, and may represent a specific nuclear matrix reconstruction appropriate for the response. ND10 protein redistribution after heat shock may be a fast-acting response until heat shock proteins exert their action by supporting processing at higher temperatures. Stores of proteins ready for immediate release may exist in ND10 and nuclear bodies. We have mostly investigated mild heat shock and can imagine the importance of such a protective mechanism for cells such as those in skin, which are exposed intermittently to high temperatures.

The redistribution of PML and the other ND10 proteins throughout the chromatin very shortly after the onset of hyperthermia is a surprising biological phenomenon. If these proteins have a function after heat shock, it is likely to take place at many sites and not at ND10. The differential distribution and relative abundance of the known ND10 proteins under various environmental conditions suggest that these proteins do not act in a stoichiometric manner and may be involved in different cellular processes.

ACKNOWLEDGMENTS

This study was supported by funds from The Wistar Institute and Core grant CA-10815 (G.G.M.) from the National Institutes of Health. We are grateful to Dr. Fu for providing MAb SC35, Dr. C. Szostecki for anti-Sp100, Dr. J.A. Dyck for anti-PML, and Dr. R. Everett for the HSV-1 mutant D22. Our thanks to Dr. J.A. Dyck for critically reading the manuscript.

REFERENCES

Ascoli CA, Maul GG (1991): Identification of a novel nuclear domain. J Cell Biol 112:785–795.

Bernstein RM (1984): Antinuclear antibodies in primary biliary cirrhosis. Lancet 1:508.

Bernstein RM, Neuberger JM, Bunn CC, Callendar ME, Hughes GRV, Williams R (1984): Diversity of autoantibodies in primary biliary cirrhosis and chronic active hepatitis. Clin Exp Immunol 55:553–560.

Bond U (1988): Heat shock but not other stress inducers leads to the disruption of a subset of snRNPs and in vitro splicing in HeLa cells. EMBO J 7:3509–3518.

Brasch K, Ochs RL (1992): Nuclear bodies (NBs): A newly "rediscovered" organelle. Exp Cell Res 202:211–223.

Carmo-Fonseca M, Pepperhole R, Carvalko MT, Lamond AJ (1992): Transcription-dependent colocalization of the U_1, U_2, U_4/U_6, and U_5 SnRNPs in coiled bodies. J Cell Biol 117:1–14.

Carter KC, Taneja KL, Lawrence JB (1991): Discrete nuclear domains of poly(A) RNA and their relationship to the functional organization of the nucleus. J Cell Biol 115: 1191–1202.

DeMaeyer EM, DeMaeyer-Guignard J (1988): "Interferons and Other Regulatory Cytokines." New York: Wiley-Interscience.

deThé G, Riviere M, Bernhard W (1960): Examen au microscope electromique de la tumeure VX2 du lapin domestique derivee du papillome de Shope. Bull Cancer 47:570–584.

deThé H, Lavan C, Marchino A, Chomienne C, Degos L, Dejean A (1991): The PML-1-RARα fusion mRNA generated by the t(15;17) translocation in acute promyelocytic leukemia encodes a functionally altered RAR. Cell 66:675–684.

Dyck JA, Maul GG, Miller WH, Chen JD, Kakizuka A, Evans RM (1994): A novel macromolecular structure is a target of the PML-RAR oncoprotein. Cell 76:333–343.

Edington BV, Whelan SA, Hightower LE (1989): Inhibition of heat shock (stress) protein induction by deuterium oxide and glycerol: Additional support for the abnormal protein hypothesis of induction. J Cell Physiol 139:219–228.

Epstein A (1984): Immunobiochemical characterization with monoclonal antibodies of Epstein-Barr virus-associated early antigens in chemically induced cells. J Virol 50:372–379.

Evans J, Reuben A, Craft J (1991): PBC 95K, a 95-kilodalton nuclear autoantigen in primary biliary cirrhosis. Arthritis Rheum 34:731–736.

Everett RD (1988): Analysis of the functional domains of herpes simplex virus type 1 immediate-early polypeptide Vmw 110. J Mol Biol 202:87–96.

Everett RD (1989): Construction and characterization of herpes simplex virus type 1 immediate early polypeptide Vmw 110. J Mol Biol 202:87–96.

Everett RD (1991): Functional and genetic analysis of the role of Vmw 110 in herpes virus replication. In Wagner EK (ed): "Herpes Virus Transcription." Boca Raton, FL: CRC Press, pp 49–76.

Everett RD, Maul GG (1995): HSV-1 IE protein Vmw 110 causes redistribution of PML. EMBO J 13:5062–5069.

Fakan S, Leser G, Martin TE (1984): Ultrastructural distribution of nuclear ribonucleoproteins as visualized by immunocytochemistry on thin sections. J Cell Biol 98:358–363.

Freundlich B, Makover D, Maul GG (1988): A novel antinuclear antibody associated with a lupus-like paraneoplastic syndrome. Ann Intern Med 109:295–297.

Fu X-D, Maniatis T (1990): Factor required for mammalian spliceosome assembly is localized to discrete regions in the nucleus. Nature 343:437–444.

Fusconi M, Cassani F, Govoni M, Caselli A, Farabegoli F, Lenzi M, Ballardini G, Zauli D, Bianchi FB (1991): Antinuclear antibodies of primary biliary cirrhosis recognize 78–92 kD and 96–100 kD proteins of nuclear bodies. J Exp Immunol 83:291–297.

Garfinkel MS, Katz MG (1993): How does influenza virus regulate gene expression at the level of mRNA translation? Let us count the ways. Gene Expr 3:109–118.

Goddard AD, Borrow J, Freemont PS, Solomon E (1991): Characterization of a zinc finger gene disrupted by the t(15;17) in acute promyelocytic leukemia. Science 254: 1371–1374.

Guldner HH, Szostecki C, Grötzinger T, Will H (1992): IFN enhances expression of Sp100, an autoantigen in primary biliary cirrhosis. J Immunol 149:4067–4073.

Harris RA, Everett RD, Zhu Z, Silverstein S, Preston CM (1989): Herpes simplex virus type-1 immediate early protein Vmw 110 reactivates latent Herpes simplex type-2 in an in vitro latency system. J Virol 63:3513–3515.

Hinglais-Guillaud N, Moricard R, Bernhard W (1961): Ultrastructure des cancers pavimenteux invasifs du col utérin chez la femme. Bull Cancer 48:283–316.

Isaacs A, Lindenmann J (1957): Virus interference. I. The interferon. Proc R Soc Lond 47:258–267.

Kakizuka A, Miller WH, Umesono K, Warrell RP, Frankel SR, Murty VV, Dmitrovsky E, Evans RM (1991): Chromosomal translocation t(15;17) in human acute promyelocytic leukemia fuses RARα with a novel putative transcription factor PML-1. Cell 66:663–674.

Kastner P, Perez A, Lutz Y, Rochette-Egly C, Gaub M-P, Durand B, Lanotte M, Berger R, Chambon P (1992): Structure, localization, and transcriptional properties of two classes of retinoic acid receptor α fusion proteins in acute promyelocytic leukemia (APL): Structure similarities with a new family of oncoproteins. EMBO J 11:629–642.

Konioth F, Gieffers C, Maul GG, Frey J (1995) Molecular characterisation of NDP52, a novel protein of the nuclear domain 10, which is redistributed upon virus infection and interferon treatment. J Cell Biol 130:1–14.

LeGoascogne C, Baulieu EE (1977): Hormonally controlled nuclear bodies during the development of prepubertal rat uterus. Biol Cell 30:195–206.

Lengyel P (1993): Tumor-suppressor genes: News about the interferon connection. Proc Natl Acad Sci USA 90:5893–5895.

Lerner MA, Boyle JA, Hardin JA, Steitz J (1981): Two novel clones of small ribonucleoproteins detected by antibodies associated with lupus erythematosus. Science 221:400–402.

Li GC, Werb Z (1982): Correlation between synthesis of heat shock proteins and development of thermotolerance in Chinese hamster fibroblasts. Proc Natl Acad Sci USA 79:3218–3222.

Maul GG (1971): On the octagonality of the nuclear pore complex. J Cell Biol 51:558–563.

Maul GG, Everett RD (1994): The nuclear location of PML, a cellular member of the C_3HC_4 zinc-binding protein family, is rearranged during herpes simplex virus infection by the C_3HC_4 viral protein ICP0. J Gen Virol 75:1223–1233.

Maul GG, Guldner HH, Spivack JG (1993): Modification of discrete nuclear domains induced by herpes virus type I immediate early gene 1 product (ICP0). J Gen Virol 74: 2679–2690.

Merrick WC (1992): Mechanism and regulation of eukaryotic protein synthesis. Microbiol Dev 56:291–315.

Milkman R (1966): Analysis of some temperature effects on *Drosophila* pupae. Biol Bull 131:331–345.

Mitchell H, Moller G, Peterson N, Lipps-Sarmients L (1979): Specific protection from phenocopy induction by heat shock. Dev Genet 1:181–192.

Padykula HA, Fitzgerald M, Clark JH, Hardin JW (1981): Nuclear bodies as structural indicators of estrogenic stimulation in uterine luminal epithelial cells. Anat Rec 201:679–696.

Pandolfi PP, Grignani F, Alcalay M, Mencarelli A, Biondi A, LoCoco F, Grignani F and Pellicci PG (1991): Structure and origins of the acute promyelocytic leukemia myc/RARα cDNA and characterization of its retinoid-binding and transactivation properties. Oncogene 6:1285–1292.

Sambrook JEF, Fritsch EF, Maniatis T (1989): "Molecular Cloning: A Laboratory Manual." Cold Spring Harbor, NY: Cold Spring Harbor Laboratory Press.

Schild D, Brake AJ, Kiefer MC, Young D, Barr PJ (1990): Cloning of three human multifunctional de novo purine biosynthetic genes by functional complementation of yeast mutations. Proc Natl Acad Sci USA 87:2916–2920.

Spector DL (1990): Higher order nuclear organization: Three-dimensional distribution of small ribonucleoprotein particles. Proc Natl Acad Sci USA 87:147–152.

Spector DL, Fu X-D, Maniatis T (1991): Association between distinct pre-mRNA splicing components and the cell nucleus. EMBO J 10:3467–3481.

Stuurman N, deGraaf A, Floore A, Josso A, Humbel B, deJong L, vanDriel R (1992): A monoclonal antibody recognizing nuclear matrix-associated nuclear bodies. J Cell Sci 101:773–784.

Szostecki C, Guldner HH, Netter HJ, Will H (1990): Isolation and characterization of cDNA encoding a human nuclear antigen predominantly recognized by autoantibodies from patients with primary biliary cirrhosis. J Immunol 145:4338–4347.

Szostecki C, Will H, Netter HJ, Guldner HH (1992): Autoantibodies to the nuclear Sp100 protein in primary biliary cirrhosis and associated diseases: Epitope specificity and immunoglobulin class distribution. Scand J Immunol 36: 555–564.

Umesono K, Evans RM (1989): Determinants of target gene specificity for steroid/thyroid hormone receptors. Cell 57: 1139–1146.

Utans U, Behrens SE, Lührmann R, Kole R, Kramer A (1992): A splicing factor that is inactivated during in vivo heat shock is functionally equivalent to the ($U_4/U_6 \cdot U_5$) triple snRNP-specific proteins. Genes Dev 6:631–641.

Weber AF, Frommes SP (1963): Nuclear bodies: Their prevalence, location, and ultrastructure in the calf. Science 141:912–913.

Weis K, Rambaud S, Lavan C, Lamond A, Dejean A (1994): Retinoic acid regulates aberrant nuclear localization of PML-RARα in acute promyelocytic leukemia cells. Cell 76:345–356.

Xie K, Lambie EY, Snyder M (1993): Nuclear dot antigens may specify transcriptional domains in the nucleus. Mol Cell Biol 13:6170–6179.

Yasuda Y, Maul GG (1990): A nucleolar autoantigen is part of a major chromosomal surface component. Chromosoma 99:153–160.

Yost HJ, Lindquist S (1986): RNA splicing is interrupted by heat shock and is rescued by heat shock protein synthesis. Cell 45:185–193.